

# Synthesis and Structures of an Unusual Germanium(II) Calix[4]arene Complex and the First Germanium(II) Calix[8]arene Complex and Their Reactivity with Diiron Nonacarbonyl

Anthony E. Wetherby, Jr.,<sup>†</sup> Lindy R. Goeller,<sup>†</sup> Antonio G. DiPasquale,<sup>‡</sup> Arnold L. Rheingold,<sup>‡</sup> and Charles S. Weinert<sup>\*†</sup>

Department of Chemistry, Oklahoma State University, Stillwater, Oklahoma 74078, and  
Department of Chemistry and Biochemistry, University of California, San Diego, La Jolla,  
California 92093-0303

Received May 18, 2007

The protonolysis reaction of the germanium(II) amide  $\text{Ge}[\text{N}(\text{SiMe}_3)_2]_2$  with calix[4]arene and calix[8]arene furnishes the two germanium(II) calixarene complexes  $\{\text{calix}[4]\}\text{Ge}_2$  and  $\{\text{calix}[8]\}\text{Ge}_4$ , respectively, which have been crystallographically characterized. The calix[4]arene complex contains a  $\text{Ge}_2\text{O}_2$  rhombus at the center of the molecule and is one of the only four germanium(II) calix[4]arenes that have been structurally characterized. The calix[8]arene species is the first reported germanium calix[8]arene complex, and it exhibits an overall bowl-shaped structure which contains two  $\text{Ge}_2\text{O}_2$  fragments. The latter complex reacts with  $\text{Fe}_2(\text{CO})_9$  to yield an octairon compound, which has also been structurally characterized and contains four  $\text{GeFe}_2$  triangles arranged around the macrocyclic ring. The germanium(II) centers are oxidized to germanium(IV) in this process, with concomitant reduction of the neutral diiron species to  $\text{Fe}_2(\text{CO})_8^{2-}$  anions.

## Introduction

Calixarenes are highly useful macrocyclic compounds which have a variable cavity size and have a variety of applications in the areas of molecular self-assembly, ionic and molecular recognition, and catalysis.<sup>1–7</sup> A number of transition-metal and main-group complexes using these species as ligands have been prepared,<sup>8–28</sup> but calixarene complexes containing germanium are rare<sup>29–35</sup> and of these

few examples only three materials having germanium bound directly to the calixarene oxygen atoms have been synthesized and structurally characterized.<sup>33,34</sup> These include the calix[4]arene complexes  $[\text{Bu}'\text{calix}]\text{Ge}_2$ <sup>33</sup> and the two struc-

\* Author to whom correspondence should be addressed. E-mail: weinert@chem.okstate.edu.

<sup>†</sup> Oklahoma State University.

<sup>‡</sup> University of California, San Diego.

- (1) Gutsche, C. D. *Calixarenes Revisited*; Royal Society of Chemistry: Cambridge, 1998.
- (2) Asfari, Z.; Böhmer, V.; Harrowfield, J.; Vincens, J., Eds. *Calixarenes 2001*; Kluwer Academic Publishers: Dordrecht, The Netherlands, 2001.
- (3) de Namor, A. F. D.; Cleverley, R. M.; Zapata-Ormachea, M. L. *Chem. Rev.* **1998**, 98, 2495–2525.
- (4) Hof, F.; Craig, S. L.; Nuckolls, C.; Rebek, J., Jr. *Angew. Chem., Int. Ed.* **2002**, 41, 1488–1508.
- (5) Pochini, A.; Ungaro, R. In *Comprehensive Supramolecular Chemistry*; Atwood, J. L.; Davis, J. E. D.; MacNicol, D. D.; Vögtle, F., Eds.; Pergamon Press: New York, 1996; Vol. 2.
- (6) Vincens, J.; Böhmer, V., Eds. *Calixarenes, A Versatile Class of Macrocyclic Compounds*; Kluwer Academic Publishers: Dordrecht, The Netherlands, 1991.
- (7) Böhmer, V. *Angew. Chem., Int. Ed.* **1995**, 34, 713–745.

- (8) Redshaw, C.; Rowan, M. A.; Warford, L.; Homden, D. M.; Arbaoui, A.; Elsegood, M. R. J.; Dale, S. H.; Yamato, T.; Casas, C. P.; Matsui, S.; Matsuura, S. *Chem.—Eur. J.* **2007**, 13, 1090–1107.
- (9) Marcos, P. M.; Mellah, B.; Ascenso, J. R.; Michel, S.; Hubscher-Bruder, V.; Arnaud-Neu, F. *New J. Chem.* **2006**, 30, 1655–1661.
- (10) Coquiere, D.; Marrot, J.; Reinaud, O. *Chem. Commun.* **2006**, 3924–3926.
- (11) Duerr, S.; Bechlars, B.; Radius, U. *Inorg. Chim. Acta* **2006**, 359, 4215–4226.
- (12) MacLachlan, E. A.; Fryzuk, M. D. *Organometallics* **2006**, 25, 1530–1543.
- (13) Jeunesse, C.; Armspach, D.; Matt, D. *Chem. Commun.* **2005**, 5603–5614.
- (14) Kotzen, N.; Goldberg, I.; Vigalok, A. *Inorg. Chem. Commun.* **2005**, 8, 1028–1030.
- (15) Sliwa, W. J. *Inclusion Phenom. Macrocyclic Chem.* **2005**, 52, 13–37.
- (16) Petrella, A. J.; Raston, C. L. *J. Organomet. Chem.* **2004**, 689, 4125–4136.
- (17) Radius, U. Z. *Anorg. Allg. Chem.* **2004**, 630, 957–972.
- (18) Dorta, R.; Shimon, L. J. W.; Rozenberg, H.; Ben-David, Y.; Milstein, D. *Inorg. Chem.* **2003**, 42, 3160–3167.
- (19) Cotton, F. A.; Daniels, L. M.; Lin, C.; Murillo, C. A. *Inorg. Chim. Acta* **2003**, 347, 1–8.
- (20) Estler, F.; Herdtweck, E.; Anwender, R. *J. Chem. Soc., Dalton Trans.* **2002**, 3088–3089.

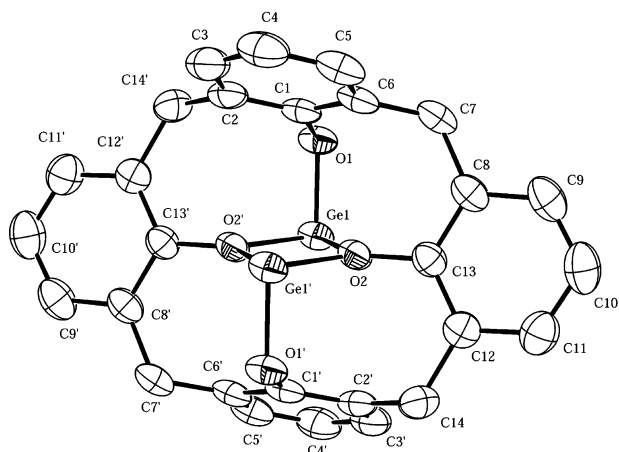


**Figure 1.** ORTEP diagram of **1**. Thermal ellipsoids are drawn at 50% probability.

tural isomers of  $[\text{Bu}'\text{calix}^{(\text{TMS})2}]\text{Ge}$ .<sup>34</sup> We have prepared the related unsubstituted germanium(II) calix[4]arene complex and also the first germanium calix[8]arene complex and have determined the X-ray crystal structures of each. All of the germanium(II) centers in both of these complexes have a lone pair of electrons available for donation to other metal centers, and thus these species could be useful platforms for the support of multiple main-group or transition-metal fragments. We have investigated the reaction of both complexes with  $\text{Fe}_2(\text{CO})_9$ , resulting in the formation of a germanium iron macrocycle containing eight iron atoms in the case of the germanium calix[8]arene compound.

## Results and Discussion

Reaction of calix[4]arene with 2 equiv of  $\text{Ge}[\text{N}(\text{SiMe}_3)_2]_2$  furnishes the cheated complex  $\{\text{calix}[4]\}\text{Ge}_2$  (**1**) in 56% yield. The structure of **1** has been determined and an ORTEP diagram is shown in Figure 1 while selected bond distances and angles are collected in Table 1. The two germanium centers are related by a center of inversion, and each is bound to three different oxygen atoms. The shorter  $\text{Ge}(1)-\text{O}(1)$  distance is representative of a typical germanium(II)–phenolic oxygen bond whereas the elongated  $\text{Ge}(1)-\text{O}(2)$  and  $\text{Ge}(1)-\text{O}(2')$  distances can be regarded as two dative

**Table 1.** Selected Bond Distances (Å) and Angles (deg) for Compound **1**

$\text{Ge}(1)-\text{O}(1)$	1.845(1)	$\text{Ge}(1)-\text{O}(2)-\text{Ge}(1')$	107.89(6)
$\text{Ge}(1)-\text{O}(2)$	1.989(1)	$\text{O}(1)-\text{Ge}(1)-\text{O}(2)$	91.72(6)
$\text{Ge}(1)-\text{O}(2')$	1.987(1)	$\text{O}(2)-\text{Ge}(1)-\text{O}(2')$	72.11(6)
$\text{C}(1)-\text{O}(1)$	1.373(3)	$\text{Ge}(1)-\text{O}(1)-\text{C}(1)$	117.9(1)
$\text{C}(13)-\text{O}(2)$	1.385(2)	$\text{Ge}(1)-\text{O}(2)-\text{C}(13)$	126.5(1)

$\text{Ge}(\text{II})-\text{O}$  bonds.<sup>36–39</sup> The germanium centers in **1** are formally in the +2 oxidation state, and the lone pairs of electrons present point out and away from the central  $\text{Ge}_2\text{O}_2$  rhombus. The  $\text{O}_{\text{term}}-\text{Ge}-\text{O}_{\text{br}}$  and bond angles in **1** are close to the expected value of  $90^\circ$ , while the angles inside the central rhombus are  $107.89(6)^\circ$  for  $\text{Ge}(1)-\text{O}(2)-\text{Ge}(1')$  and  $72.11(6)^\circ$  for  $\text{O}(2)-\text{Ge}(1)-\text{O}(2')$ . The aromatic ring attached to the  $\text{O}(1)$  atom is bent back such that they lie above  $\text{Ge}(1')$  on the opposite side of the  $\text{Ge}_2\text{O}_2$  rhombus, and the closest contact between the ring carbons and the germanium atoms is  $3.28 \text{ \AA}$  indicating the absence of any  $\text{Ge}-\text{C}$   $\pi$ -type interactions.

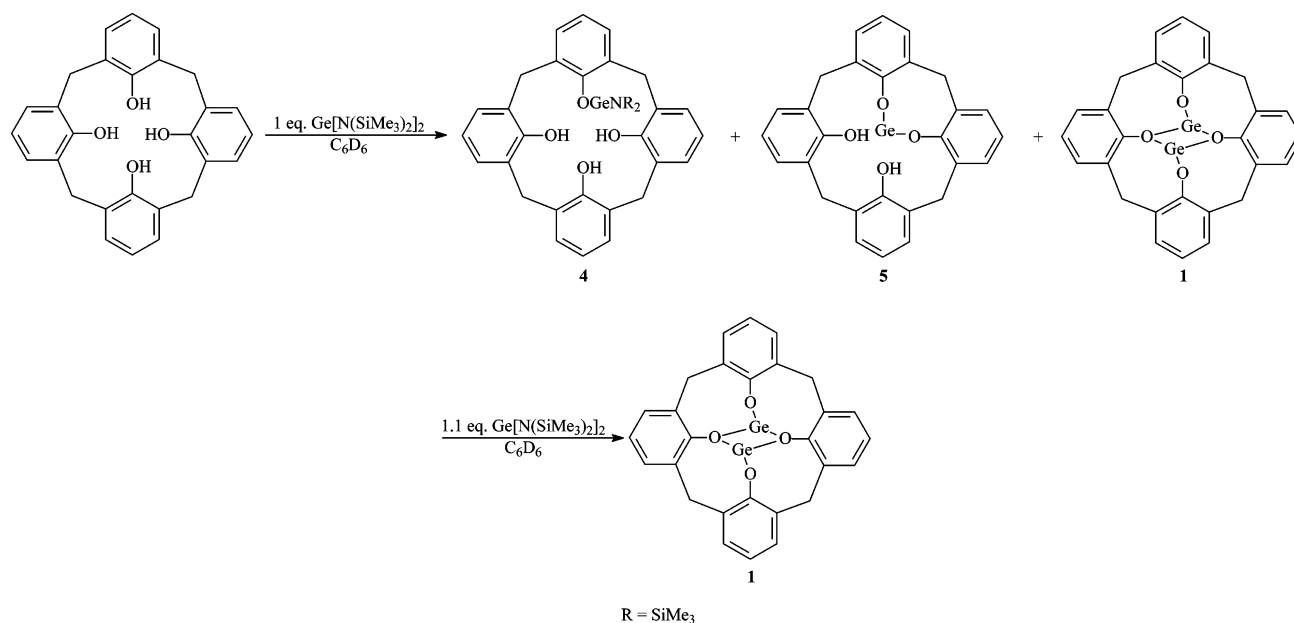
The bonding environment in the  $\text{Ge}_2\text{O}_2$  rhombus closely resembles that of the germanium(II) aryloxide compounds  $[\text{Ge}(\text{OC}_6\text{H}_3(\text{Pr}^i)_2-2,6)_2]_2$  and  $[\text{Ge}(\text{OC}_6\text{H}_2(\text{Me})_3-2,4,6)_2]_2$ , both of which contain bridging aryloxide groups.<sup>38</sup> Furthermore, the structures of **1** and the *tert*-butyl calix[4]arene  $[\text{Bu}'\text{calix}]\text{Ge}_2$  (**2**)<sup>33</sup> are nearly identical with these two species having the same  $\text{Ge}-\text{O}$  bond distances and  $\text{O}-\text{Ge}-\text{O}$  bond angles within the measured estimated standard deviation values. The structures of the two possible isomers of the only other crystallographically characterized germanium(II) calixarene  $[\text{Bu}'\text{calix}^{(\text{TMS})2}]\text{Ge}$  (**3**) differ considerably from **1** and **2** in that **3** contains only one germanium atom and can adopt either an exo or an endo isomeric form.<sup>34</sup> In the exo isomer, the germanium atom is formally bound to the two unsubstituted oxygen atoms with  $\text{Ge}-\text{O}$  distances of  $1.765(6)$  and  $1.842(6) \text{ \AA}$  and also exhibits long dative interactions with the oxygen atoms of the two  $-\text{OSiMe}_3$  groups measuring  $2.421(5)$  and  $2.486(5) \text{ \AA}$ . In the endo isomer, the  $\text{Ge}-\text{O}$  distances are  $1.841(5)$  and  $1.853(5) \text{ \AA}$  and there are no dative interactions with the oxygen atoms of the trimethylsiloxy groups. The formal  $\text{Ge}-\text{O}$  single bonds in the endo isomer are similar to those of **1**, while the elongated dative interactions are a result of the steric crowding of the  $-\text{OSiMe}_3$  groups which point outward from the center of the macrocycle.

While free calix[4]arene undergoes a rapid exchange between a cone and inverted cone configuration in solution,<sup>40</sup> the presence of the bridging oxygen atoms attached to the two germanium centers enforces structural rigidity in **1**. The  $^1\text{H}$  NMR spectrum obtained for **1** correlates with its solid-state structure, where resonances for protons directed toward

- (21) Sliwa, W. *Croat. Chem. Acta* **2002**, 75, 131–153.
- (22) Seitz, J.; Maas, G. *Chem. Commun.* **2002**, 338–339.
- (23) Brown, M.; Jablonski, C. *Can. J. Chem.* **2001**, 79, 463–471.
- (24) Löffler, F.; Luning, U.; Gohar, G. *New J. Chem.* **2000**, 24, 935–938.
- (25) Pellet-Rostaing, S.; Regnoud-de-Vains, J.-B.; Lamartine, R.; Fenet, B. *Inorg. Chem. Commun.* **1999**, 2, 44–47.
- (26) Xie, D.; Gutsche, C. D. *J. Org. Chem.* **1998**, 63, 9270–9278.
- (27) Khasnis, D. V.; Burton, J. M.; Lattman, M.; Zhang, H. *J. Chem. Soc., Chem. Commun.* **1991**, 562–563.
- (28) Khasnis, D. V.; Lattman, M.; Gutsche, C. D. *J. Am. Chem. Soc.* **1990**, 112, 9422–9423.
- (29) Sakurai, T.; Takeuchi, Y. *Appl. Organomet. Chem.* **2005**, 19, 372–376.
- (30) Sakurai, T.; Takeuchi, Y. *Appl. Organomet. Chem.* **2004**, 18, 23–27.
- (31) Sakurai, T.; Takeuchi, Y. *Heteroat. Chem.* **2003**, 14, 365–373.
- (32) Takeuchi, Y.; Sakurai, T.; Tanaka, K. *Main Group Met. Chem.* **2000**, 23, 311–316.
- (33) McBurnett, B. G.; Cowley, A. H. *Chem. Commun.* **1999**, 17–18.
- (34) Hascall, T.; Rheingold, A. L.; Guzei, I.; Parkin, G. *Chem. Commun.* **1998**, 101–102.
- (35) Hockemeyer, J.; Valentin, B.; Castel, A.; Riviere, P.; Satge, J.; Cardin, C. J.; Teixeira, S. *Main Group Met. Chem.* **1997**, 20, 775–781.

- (36) Weinert, C. S.; Fanwick, P. E.; Rothwell, I. P. *J. Chem. Soc., Dalton Trans.* **2002**, 2948–2950.
- (37) Weinert, C. S.; Fanwick, P. E.; Rothwell, I. P. *Acta Crystallogr.* **2002**, E58, m718–m720.
- (38) Weinert, C. S.; Fenwick, A. E.; Fanwick, P. E.; Rothwell, I. P. *J. Chem. Soc., Dalton Trans.* **2003**, 532–539.
- (39) Weinert, C. S.; Fanwick, P. E.; Rothwell, I. P. *Inorg. Chem.* **2003**, 42, 6089–6094.
- (40) Lang, J.; Deckerová, V.; Czernek, J.; Lhoták, P. *J. Chem. Phys.* **2005**, 122, 0445061–04450611.

Scheme 1



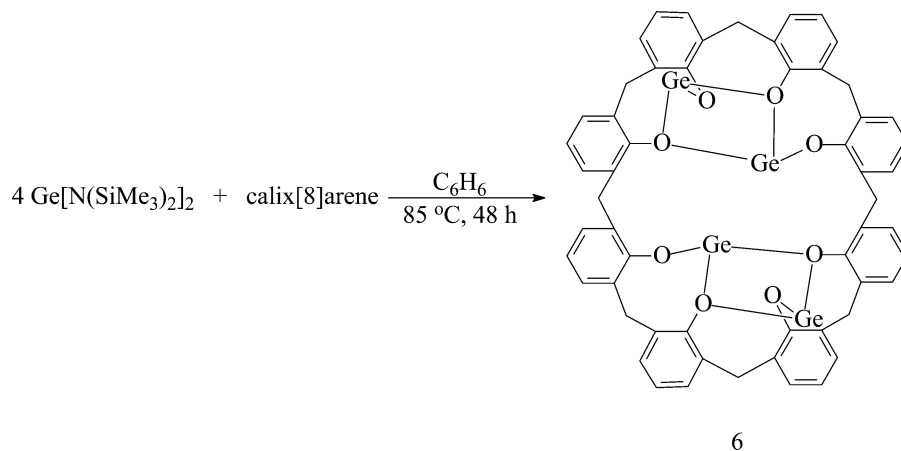
the central Ge<sub>2</sub>O<sub>2</sub> rhombus are shifted downfield versus those pointing away from this moiety, which are observed for both the *meta* and *para* protons of the aromatic rings. The two sets of bridging methylene units of the calix[4]arene ligand system are also diastereotopic, where the protons attached to C(7) and C(14) directed toward the Ge<sub>2</sub>O<sub>2</sub> rhombus give rise to a doublet at  $\delta$  4.41 ppm ( $J$  = 12.9 Hz) whereas those attached to these two carbon atoms and directed away from the Ge<sub>2</sub>O<sub>2</sub> fragment appear as a doublet at  $\delta$  3.23 ppm ( $J$  = 12.9 Hz).

The pathway for the formation of **1** was determined to occur in a stepwise manner and was monitored using <sup>1</sup>H NMR spectroscopy by the introduction of sequential aliquots of Ge[N(SiMe<sub>3</sub>)<sub>2</sub>]<sub>2</sub> to a solution of calix[4]arene in C<sub>6</sub>D<sub>6</sub>. The diagnostic resonances for this investigation were those of the bridging methylene units as well as the hydroxyl resonances of the calix[4]arene system. Calix[4]arene exhibits a singlet at  $\delta$  10.21 ppm in C<sub>6</sub>D<sub>6</sub> arising from the four equivalent hydroxyl protons, and the methylene resonances for this compound appear as two broad features centered at  $\delta$  4.12 and 3.28 ppm due to the rapid interconversion of the

macrocyclic ring system from a cone to an inverted cone configuration<sup>40</sup> and correspond to the axial and equatorial –CH<sub>2</sub>– groups, respectively.

Addition of 1 equiv of Ge[N(SiMe<sub>3</sub>)<sub>2</sub>]<sub>2</sub> to a C<sub>6</sub>D<sub>6</sub> solution of calix[4]arene results in the formation of two intermediate species as well as the final product **1** (Scheme 1). Two singlets for the nonequivalent –OH groups of **4** were visible at  $\delta$  9.50 and 9.18 ppm (intensity ratio 1:2), while a third singlet at  $\delta$  7.74 ppm arises from the two equivalent –OH groups of **5**. The integrated intensity of the feature for **5** was approximately half of that of the two resonances for **4**. The feature at  $\delta$  10.21 ppm for the calix[4]arene starting material was also still present. The formation of **4** and **5** was also reflected in the signals for the methylene groups of the calix[4]arene system as there were six sets of doublets visible in the <sup>1</sup>H NMR spectrum at this time. The signals at  $\delta$  4.41 and 3.23 ppm correspond to **1**, those at  $\delta$  4.38 ( $J$  = 12.9 Hz) and 3.26 ( $J$  = 13.8 Hz) ppm correspond to **4**, and those at  $\delta$  4.33 ( $J$  = 13.8 Hz) and 3.18 ( $J$  = 13.5 Hz) ppm correspond to **5**, wherein the assignments for **4** and **5** are based on the integrated intensities of the respective peaks. A singlet at  $\delta$  0.90 ppm was also visible due to the formation

Scheme 2



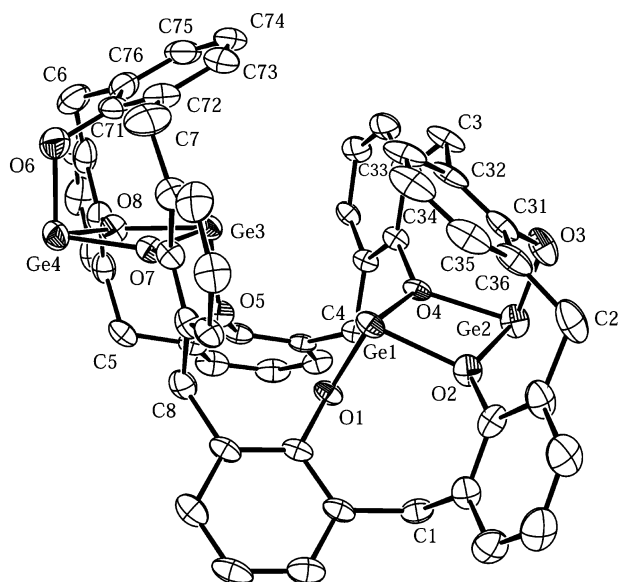


**Figure 2.** ORTEP diagram of  $6 \cdot C_6H_6$ . The benzene molecule is not shown, and thermal ellipsoids are drawn at 50% probability.

**Table 2.** Selected Bond Distances (Å) and Angles (deg) for Compound  $6 \cdot C_6H_6$

Ge(1)—O(1)	1.834(4)	O(1)—Ge(1)—O(2)	93.7(2)
Ge(1)—O(2)	2.036(3)	O(1)—Ge(1)—O(4)	90.7(1)
Ge(1)—O(4)	2.012(3)	O(2)—Ge(1)—O(4)	72.0(1)
Ge(2)—O(2)	1.970(3)	O(2)—Ge(2)—O(3)	94.4(2)
Ge(2)—O(3)	1.833(4)	O(3)—Ge(2)—O(4)	92.3(2)
Ge(2)—O(4)	2.000(3)	O(2)—Ge(2)—O(4)	73.6(1)
Ge(3)—O(5)	1.837(4)	O(5)—Ge(3)—O(7)	93.0(2)
Ge(3)—O(7)	2.019(3)	O(5)—Ge(3)—O(8)	92.1(2)
Ge(3)—O(8)	2.030(3)	O(7)—Ge(3)—O(8)	71.7(1)
Ge(4)—O(6)	1.828(4)	O(6)—Ge(4)—O(7)	95.2(2)
Ge(4)—O(7)	1.980(3)	O(6)—Ge(4)—O(8)	93.1(2)
Ge(4)—O(8)	1.953(4)	O(7)—Ge(4)—O(8)	74.2(1)
		Ge(1)—O(2)—Ge(2)	106.5(1)
		Ge(1)—O(4)—Ge(2)	106.3(1)
		Ge(3)—O(7)—Ge(4)	106.1(1)
		Ge(3)—O(8)—Ge(4)	106.7(1)

of  $HN(SiMe_3)_2$ , and a singlet at  $\delta$  0.28 ppm can be attributed to the trimethylsilyl groups of **4**. Addition of a further 0.5 equiv of  $Ge[N(SiMe_3)_2]_2$  to the NMR tube resulted in an increase in intensity of the hydroxyl resonance at  $\delta$  7.74 ppm for **5**, while the hydroxyl resonances for **4** and calix[4]arene were very weak. The methylene resonances for **4** had also diminished, while those for **1** and **5** had increased in intensity. Increasing the amount of  $Ge[N(SiMe_3)_2]_2$  to a slight excess of 2 equiv resulted in the consumption of the remaining calix[4]arene starting material and complete conversion of **4** and **5** to compound **1**.

The reaction of calix[8]arene with 4 equiv of  $Ge[N(SiMe_3)_2]_2$  resulted in the formation of the tetragermanium species {calix[8]} $Ge_4$  (**6**) in excellent (89%) yield (Scheme 2). The structure of  $6 \cdot C_6H_6$  was determined and an ORTEP diagram is shown in Figure 2, while selected bond distances and angles are collected in Table 2. The four germanium atoms in **6** are assembled in pairs on opposite sides of the molecule, and each germanium is bound to three oxygen atoms to form rhombi in a similar fashion to **1**. The Ge—O bonds to the terminal oxygen atoms are all shorter than those to the bridging oxygens with an average value of

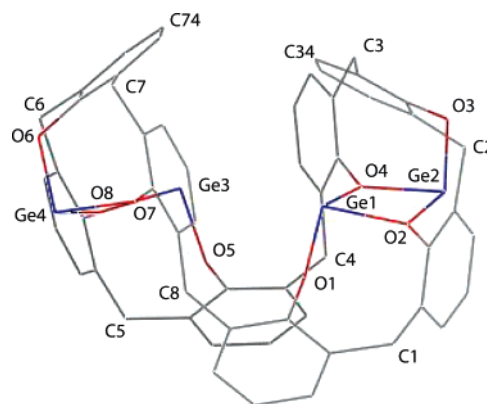


**Figure 3.** Wireframe drawing of **6**. The germanium atoms are drawn in blue, the oxygen atoms in red, and the carbon atoms in gray.

1.833(4) Å, which is considerably shorter than the corresponding distances in **1**.

Both of the  $Ge_2O_2$  rhombi in **6** have essentially the same geometry wherein the individual fragments are skewed such that one Ge—O<sub>br</sub> distance is shorter than the other for each of the four germanium atoms (Table 2). The O<sub>term</sub>—Ge—O<sub>br</sub> bond angles deviate significantly from 90° with an average value of 93.1(2)° while the O<sub>br</sub>—Ge—O<sub>br</sub> angles within the  $Ge_2O_2$  rhombi have an average value of 72.9(2)°, and the average Ge—O<sub>br</sub>—Ge bond angle within the  $Ge_2O_2$  fragments is 106.4(1)°. The Ge(1)—O(2)—Ge(2)—O(4) rhombus is puckered by 8.2° while the other fragment containing Ge(3)—O(7)—Ge(4)—O(8) is puckered by 7.3°. This contrasts with the structure of **1** where the  $Ge_2O_2$  moiety is completely planar. The overall shape of the molecule resembles a deep U-shaped bowl with two of the aromatic rings, which contain C(31)—C(36) and C(71)—C(76), bent inward toward the center of the molecule. A wireframe diagram illustrating the structure of the molecule is shown in Figure 3.

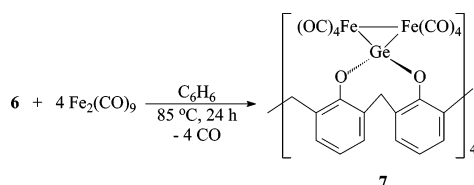
As found for **1**, the individual protons of the eight methylene groups in the calix[8]arene macrocycle are magnetically nonequivalent and the presence of an approximate center of symmetry in the molecule results in the appearance of eight doublets for these protons in the  $^1H$  NMR spectrum of **6**. One resonance appears far downfield at  $\delta$  5.83 ppm ( $J$  = 16.8 Hz) that can be attributed to the hydrogen atoms H(4a) and H(8a) bound to C(4) and C(8), which are located at the bottom of the bowl-shaped geometry of the molecule and point inward toward each of the two  $Ge_2O_2$  rhombi. In the solid-state structure of **6**, H(8a) has two close contacts with O(1) and O(5) measuring 2.32(1) and 2.52(1) Å, respectively, while H(4a) has two similar close contacts with O(1) and O(4) measuring 2.32(1) and 2.46(1) Å, respectively, all of which are within the sum of the van der Waals radii of hydrogen and oxygen (2.60 Å).<sup>41</sup> There are two additional close contacts between H(4a)—O(5) and H(8a)—O(1) measuring 2.67(1) and 2.60(1) Å, respectively.

The hydrogen atom H(1b) has two close contacts with O(1) (2.48(1) Å) and O(2) (2.47(1) Å), and H(5b) has close contacts with O(5) and O(8) measuring 2.52(1) and 2.50(1) Å, respectively. These two protons, which are directed inward

(41) Emsley, J. *The Elements*, 2nd ed.; Clarendon Press: Oxford, 1991.



Scheme 3



toward the  $\text{Ge}_2\text{O}_2$  rhombi, result in the appearance of a doublet at  $\delta$  4.77 ppm ( $J = 12.6$  Hz) in the  $^1\text{H}$  NMR spectrum of **6**, and a second set of closely spaced doublets at  $\delta$  4.60 ( $J = 15.8$  Hz) and 4.57 ( $J = 15.0$  Hz) ppm can be attributed to the four protons attached to C(2) and C(3) and C(6) and C(7), respectively, which are directed inward toward the two  $\text{Ge}_2\text{O}_2$  rhombi. The remaining eight hydrogen atoms on each of the methylene groups are directed outward from the two  $\text{Ge}_2\text{O}_2$  rhombi and have chemical shifts in the range of  $\delta$  3.48–3.22 ppm. One feature appears upfield at  $\delta$  3.24 ppm ( $J = 12.6$  Hz) arising from the two protons attached to C(1) and C(5) which are located at distances of 4.46 and 4.47 Å, respectively, from the centroids of the two  $\text{Ge}_2\text{O}_2$  rhombi in **6**.

The presence of four lone pairs of electrons on the germanium(II) atoms in **6** renders this molecule a potentially useful platform for the support of multiple coordinatively unsaturated transition-metal centers. In order to investigate this postulate, compound **6** was reacted with 4 equiv of  $\text{Fe}_2(\text{CO})_9$  resulting in the isolation of a ruby-red solid in good (73%) yield (Scheme 3). The product was isolated and identified to be the octairon complex **7** upon obtaining its X-ray crystal structure. Compound **7** crystallizes with one molecule of benzene in the unit cell and an ORTEP diagram of **7** is shown in Figure 4, while selected bond distances and angles are collected in Table 3. The overall complex has fourfold symmetry, and the entire structure can be

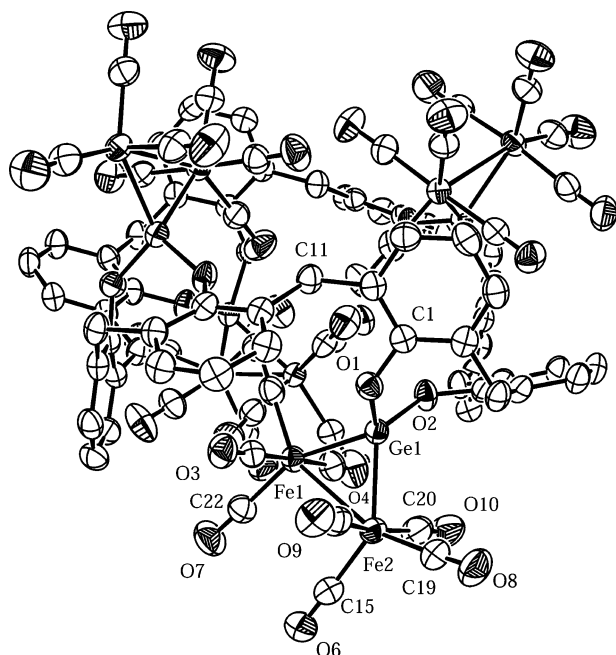


**Figure 4.** ORTEP diagram of the complete molecule of **7**· $\text{C}_6\text{H}_6$ . The benzene molecule is not shown, and thermal ellipsoids are drawn at 50% probability.

**Table 3.** Selected Bond Distances (Å) and Angles (deg) for Compound **7**· $\text{C}_6\text{H}_6$

Ge(1)–O(1)	1.788(2)	O(1)–Ge(1)–O(2)	103.7(1)
Ge(1)–O(2)	1.772(2)	O(1)–Ge(1)–Fe(1)	116.77(7)
Ge(1)–Fe(1)	2.3543(5)	O(1)–Ge(1)–Fe(2)	119.70(7)
Ge(1)–Fe(2)	2.3244(6)	O(2)–Ge(1)–Fe(1)	115.91(7)
Fe(1)–Fe(2)	2.8407(6)	O(2)–Ge(1)–Fe(2)	124.55(8)
Fe(1)–C(16)	1.812(3)	Fe(1)–Ge(1)–Fe(2)	74.77(2)
Fe(1)–C(17)	1.810(4)	Ge(1)–Fe(1)–Fe(2)	52.14(2)
Fe(1)–C(18)	1.778(4)	Ge(1)–Fe(2)–Fe(1)	53.10(2)
Fe(1)–C(22)	1.826(4)	Ge(1)–Fe(1)–C(16)	90.6(1)
Fe(2)–C(15)	1.837(4)	Ge(1)–Fe(1)–C(17)	90.0(1)
Fe(2)–C(19)	1.791(4)	Ge(1)–Fe(1)–C(18)	96.3(1)
Fe(2)–C(20)	1.808(4)	Ge(1)–Fe(1)–C(22)	154.5(1)
Fe(2)–C(21)	1.806(4)	Ge(1)–Fe(2)–C(15)	140.5(1)
C(15)–O(6)	1.120(5)	Ge(1)–Fe(2)–C(19)	108.0(1)
C(16)–O(3)	1.131(4)	Ge(1)–Fe(2)–C(20)	85.9(1)
C(17)–O(4)	1.129(5)	Ge(1)–Fe(2)–C(21)	87.6(1)
C(18)–O(5)	1.150(4)		
C(19)–O(8)	1.125(5)		
C(20)–O(10)	1.140(5)		
C(21)–O(9)	1.139(5)		
C(22)–O(7)	1.121(4)		

generated from the asymmetric unit which consists of a germanium atom, a  $\text{Fe}_2(\text{CO})_8$  moiety, two phenyl rings, and two methylene groups. The structure of this fragment is shown in Figure 5.

Initially, we expected the reaction of **6** with  $\text{Fe}_2(\text{CO})_9$  to result in cleavage of the Fe–Fe bond leading to the coordination of a  $\text{Fe}(\text{CO})_4$  unit to each of the germanium centers with concomitant formation of free  $\text{Fe}(\text{CO})_5$ , which was observed in the reaction of  $(\text{Bu}'_2\text{-2,6-Me-4-C}_6\text{H}_2\text{O})_2\text{Ge}$  with  $\text{Fe}_2(\text{CO})_9$ .<sup>42</sup> Instead, reductive decarbonylation involving extrusion of one bridging CO group in  $\text{Fe}_2(\text{CO})_9$  and formation of four triangular  $\text{GeFe}_2$  three-membered rings was observed. This reaction involves formal oxidation of the Ge atoms from the +2 to the +4 oxidation state as the diiron fragments are regarded as  $\text{Fe}_2(\text{CO})_8^{2-}$  anions. The difference in the reactivity between **6** and germylene complex with  $\text{Fe}_2(\text{CO})_9$  likely stems from the electronic attributes of the  $\text{Ge}_2\text{O}_2$  moieties versus a discrete germanium(II) atom in  $(\text{Bu}'_2\text{-2,6-Me-4-C}_6\text{H}_2\text{O})_2\text{Ge}$ . The oxidation state of germanium is clearly indicated by the Ge–O distances in **7**, which measure 1.772(2) and 1.788(2) Å and are representative of Ge(IV)–O single bonds. Each germanium center is, thus, formally bound to two oxygen atoms and any dative-type interactions are absent, which is expected since germanium(IV) does not have the vacant p-orbital that can accommodate electron density from donor atoms or molecules; the p-orbital is available when it is in the +2 oxidation state.

Formation of **7** also results in the reduction of each of the iron atoms of  $\text{Fe}_2(\text{CO})_9$  from the neutral to the -1 formal oxidation state with loss of one carbonyl ligand. Thus, the reaction of  $\text{Fe}_2(\text{CO})_9$  with the germanium atoms of the calix-[8]arene complex can be regarded as a two-electron transfer from each of the four germanium centers to a bonded pair of iron atoms to generate the di-ferrate moiety. The  $\text{GeFe}_2$  triangles are planar, and each of the iron atoms in these groups has approximate  $C_s$  symmetry. The iron–iron bond

(42) Hitchcock, P. B.; Lappert, M. F.; Thomas, S. A.; Thorne, A. J.; Carty, A. J.; Taylor, N. J. *J. Organomet. Chem.* **1986**, 315, 27–44.

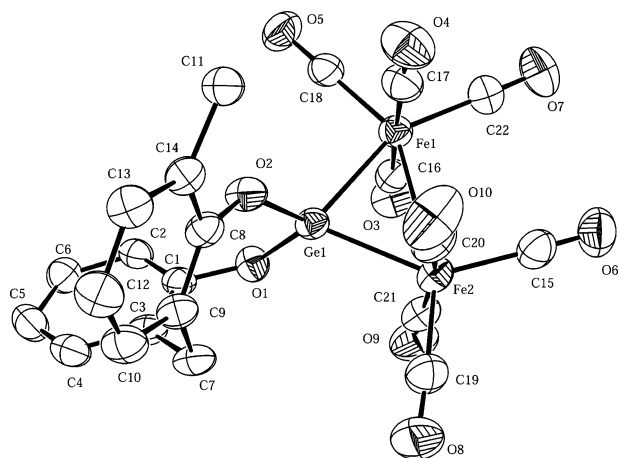


**Figure 5.** ORTEP diagram of the asymmetric unit of  $7 \cdot \text{C}_6\text{H}_6$ . Thermal ellipsoids are drawn at 50% probability.

length in **7** is 2.8407(6) Å while the two Ge–Fe distances measure 2.3543(5) and 2.3244(6) Å. The Fe–Fe distance in the dianion of  $[(\text{Ph}_3\text{P})_2\text{N}]_2[\text{Fe}_2(\text{CO})_8] \cdot 2\text{CH}_3\text{CN}$  is 2.787(2) Å,<sup>43</sup> which like **7** has no bridging carbonyl ligands. The introduction of a  $\mu_2$ -bridging germanium(IV) atom results in an elongation of the Fe–Fe bond due to electron donation from the  $\text{Fe}_2(\text{CO})_8^{2-}$  anion to the germanium(IV) metal center.

The germanium atoms of **7** are in a highly distorted tetrahedral environment enforced by the presence of the  $\text{GeFe}_2$  moieties. The O(1)–Ge(1)–O(2) angle is compressed to 103.7(1)° from the ideal value of 109.5°, and the two O–Ge–Fe angles are widened to 119.70(7)° and 124.55(8)°. The Fe(1)–Ge(1)–Fe(2) angle is highly distorted from the ideal value measuring 74.77(2)°. The geometry at the germanium centers is a result of the presence of the strained  $\text{GeFe}_2$  triangles, and the bond angles within these groups are also significantly distorted from their ideal values of 60°. The internal angles in the  $\text{GeFe}_2$  triangles measure 52.14(2)°, 53.10(2)°, and 74.77(2)° for the Ge(1)–Fe(1)–Fe(2), Ge(1)–Fe(2)–Fe(1), and Fe(1)–Ge(1)–Fe(2) angles, respectively, indicating the presence of significant angle strain in these moieties.

The spirocyclic complex  $\text{Ge}[\text{Fe}_2(\text{CO})_8]_2$  (**8**)<sup>44–46</sup> contains two  $\text{Fe}_2(\text{CO})_8^{2-}$  groups bridged by a bare germanium atom, and the structure of **8** has been reported on two separate occasions.<sup>44,45</sup> The two reported structures that were determined are nearly identical, with one having an average Ge–Fe distance of 2.40(1) Å and an average Fe–Fe bond length of 2.823(2) Å<sup>44</sup> and the other having average Ge–Fe and Fe–Fe distances of 2.407(2) and 2.823(3) Å, respectively.<sup>45</sup> The longer Ge–Fe and shorter Fe–Fe distances in **8** versus those in **7** are likely a result of the attachment of the two germanium atoms in **7** to electron-withdrawing phenolic

oxygen atoms versus a second  $\text{Fe}_2(\text{CO})_8^{2-}$  moiety in **8**. The average Fe–Ge–Fe bond angle in **8** (among the two structure reports) is 71.9(1)° while the average Ge–Fe–Fe bond angle is 54.0(1)°,<sup>44,45</sup> both of which are more acute than the corresponding angles in **7** due to the spirocyclic geometry in **8**.

The geometries at the iron atoms in **7** and **8** are identical but the C–O bond lengths in **7** are shorter than the corresponding distances in **8**,<sup>44</sup> again resulting from the germanium atoms in **7** being bound to electron-withdrawing phenolic oxygen atoms. The average of the bond distances for the C–O groups pointing outward from the  $\text{GeFe}_2$  triangle (C(15)–O(6) and C(22)–O(7)) in **7** is 1.120(4) Å while the corresponding C–O groups for **8** have an average distance of 1.134(7) Å.<sup>44</sup> The three sets of C–O distances remaining in **7** average 1.135(4), 1.140(4), and 1.132(4) Å while the corresponding average distances in **8** are 1.140(7), 1.138(7), and 1.148(7) Å.<sup>44</sup>

These differences are manifested in the infrared spectrum of **7** in  $\text{CH}_2\text{Cl}_2$ , which contains four carbonyl stretching bands at 2109, 2059, 2044, and 2020  $\text{cm}^{-1}$  as a result of the  $C_s$  symmetry at each of the iron atoms. Each of these bands appear at higher energy than the corresponding IR features for **8** in  $\text{CH}_2\text{Cl}_2$  (2076, 2050, 2033, and 2011  $\text{cm}^{-1}$ ).<sup>45</sup> These structural and spectroscopic differences indicate that the C–O bonds in **7** are stronger than those in **8** since the  $\text{Fe}_2(\text{CO})_8^{2-}$  groups in **7** are more strongly bound to the germanium atom than those in **8**, which results in less electron density for Fe–CO backbonding to the carbonyl groups.

The  $^1\text{H}$  NMR spectrum of **7** recorded in  $\text{CD}_3\text{CN}$  indicates that the molecule retains its rigid structure in solution. There are four doublets for each of the magnetically nonequivalent methylene protons of **7** as also found in the  $^1\text{H}$  NMR spectra of compounds **1** and **6**. A resonance at  $\delta$  4.70 ppm ( $J$  = 10.2 Hz) arises from the protons attached to C(7) which are directed toward the  $\text{GeFe}_2$  triangles while that at  $\delta$  3.42 ppm ( $J$  = 10.2 Hz) corresponds to the protons on C(7) which are directed away from this fragment. The other two doublets at  $\delta$  4.12 ( $J$  = 12.9 Hz) and 3.72 ppm ( $J$  = 12.9 Hz) are assigned to the protons attached to C(11), which are directed toward and away from the  $\text{GeFe}_2$  triangles, respectively.

Several other carbonyl compounds containing the  $\text{GeFe}_2$  structural motif have been reported and characterized<sup>47–52</sup> as have complexes containing  $\text{GeCo}_2$  triangles.<sup>53–59</sup> In addition, a number of higher nuclearity clusters containing  $\mu_3$ -<sup>60–63</sup> or  $\mu_4$ -germanium atoms,<sup>53–55,64–68</sup>  $\text{Ge}_2\text{Fe}_2$  arrays,<sup>69–71</sup>

(43) Chin, H. B.; Smith, M. B.; Wilson, R. D.; Bau, R. *J. Am. Chem. Soc.* **1974**, 96, 5285–5287.

(44) Batsanov, A. S.; Rybin, L. V.; Rybinskaya, M. I.; Struchkov, Y. T.; Salimgareev, I. M.; Bogatova, N. G. *J. Organomet. Chem.* **1983**, 249, 319–326.

(45) Melzer, D.; Weiss, E. *J. Organomet. Chem.* **1983**, 255, 335–344.

(46) Anema, S. G.; Barris, G. C.; Mackay, K. M.; Nicholson, B. K. *J. Organomet. Chem.* **1988**, 350, 207–215.

(47) Anema, S. G.; Mackay, K. M.; Nicholson, B. K. *Inorg. Chem.* **1989**, 28, 3158–3164.

(48) Anema, S. G.; Mackay, K. M.; McLeod, L. C.; Nicholson, B. K.; Whittaker, J. M. *Angew. Chem., Int. Ed. Engl.* **1986**, 25, 759–760.

(49) Mohamed, B. A. S.; Kikuchi, M.; Hashimoto, H.; Ueno, K.; Tobita, H.; Ogino, H. *Chem. Lett.* **2004**, 33, 112–113.

(50) Kawano, Y.; Sugawara, K.; Tobita, H.; Ogino, H. *Chem. Lett.* **1994**, 293–296.

(51) Bonny, A.; Mackay, K. M.; Wong, F. S. *J. Chem. Res., Synop.* **1985**, 40–41.

(52) Bonny, A.; Mackay, K. M. *J. Chem. Soc., Dalton Trans.* **1978**, 722–726.

or rings containing germanium, iron, and cobalt<sup>62,72–75</sup> are also known. The synthesis of these species typically involves using germanium(IV) precursors, while preparative routes involving the oxidation of germanium(II) precursors such as that employed for the synthesis of **7** are more uncommon. One notable exception is the synthesis of  $[\text{Et}_4\text{N}]_2[\text{Fe}_3(\text{CO})_9(\mu_3\text{-CO})(\mu_3\text{-Ge}\{\text{Fe}(\text{CO})_4\})]$  from  $[\text{Et}_4\text{N}]_2[\text{Fe}_2(\text{CO})_8]$  and  $\text{GeI}_2$ .<sup>60</sup> Reaction of **1** with 2 equiv of  $\text{Fe}_2(\text{CO})_9$  neither furnished a complex similar to **7** nor resulted in the formation of  $\text{Ge}-\text{Fe}(\text{CO})_4$  fragments. Although a reaction did occur, the products were identified as **1** and fine particles of iron metal. Presumably, the decarbonylation of  $\text{Fe}_2(\text{CO})_9$  by complex **1** results in an unstable species, which releases all of the remaining carbonyl ligands to furnish the iron metal.

## Conclusions

We have prepared and structurally characterized two unusual germanium(II) calixarene complexes via the protonolysis reaction between the bulky germanium(II) amide  $\text{Ge}[\text{N}(\text{SiMe}_3)_2]_2$  and calix[4]arene or calix[8]arene. The former complex is highly symmetric and contains two germanium atoms arranged in a central  $\text{Ge}_2\text{O}_2$  rhombus, while the latter species represents the first germanium(II)–calix[8]arene complex that contains two of these  $\text{Ge}_2\text{O}_2$  rhombi located inside a bowl-shaped macrocycle. The latter complex reacts

with  $\text{Fe}_2(\text{CO})_9$  to give a highly symmetric octairon complex containing four  $\text{GeFe}_2$  triangles attached to the macrocyclic calix[8]arene framework. This process indicates that these germanium(II) calixarenes can serve as platforms for the support of multiple transition-metal centers.

## Experimental Section

**General Considerations.** All manipulations were carried out under an inert  $\text{N}_2$  atmosphere using standard glovebox, Schlenk, and syringe techniques.<sup>76</sup> Solvents were dried and purified using a Glass Contour solvent purification system. Calix[4]arene, calix[8]arene, and  $\text{Fe}_2(\text{CO})_9$  were purchased from Aldrich and used without further purification, and  $\text{Ge}[\text{N}(\text{SiMe}_3)_2]_2$  was prepared according to the literature method.<sup>77–79</sup> Infrared spectra were obtained using a Hewlett-Packard FT-IR spectrometer, and NMR spectra were recorded on either a Varian Gemini 2000 or a Varian Unity INOVA 400 operating at 300 or 400 MHz, respectively, and were referenced to residual protio solvent. The numbering system used below refers to that in the crystal structures of **1**, **6**, and **7**.

**Synthesis of {Calix[4]} $\text{Ge}_2$  (**1**).** To a solution of calix[4]arene (0.404 g, 0.952 mmol) in benzene (25 mL) in a Schlenk tube was added a solution of  $\text{Ge}[\text{N}(\text{SiMe}_3)_2]_2$  (0.750 g, 1.91 mmol) in benzene (5 mL). The tube was sealed with a Teflon plug, and the reaction was heated at 85 °C in an oil bath for 24 h. The volatiles were removed in vacuo to yield an off-white solid, which was washed with hexane ( $3 \times 5$  mL) and subsequently recrystallized from hot benzene (10 mL) to yield **1** (0.301 g, 56%) as colorless crystals. <sup>1</sup>H NMR ( $\text{C}_6\text{D}_6$ , 25 °C):  $\delta$  7.07 (d,  $J = 7.5$  Hz, 4H, *meta*-H C(1)–C(6)), 6.86 (t,  $J = 7.5$  Hz, 2H, *para*-H C(1)–C(6)), 6.68 (d,  $J = 7.5$  Hz, 4H, *meta*-H C(8)–C(13)), 6.16 (d,  $J = 7.5$  Hz, 2H, *para*-H C(8)–C(13)), 4.41 (d,  $J = 12.9$  Hz, 4H,  $-\text{C}(7)\text{H}_2-$ ), 3.23 (d,  $J = 12.9$  Hz, 4H,  $-\text{C}(14)\text{H}_2-$ ) ppm.

**Stepwise Reaction of  $\text{Ge}[\text{N}(\text{SiMe}_3)_2]_2$  with Calix[4]arene.** To a solution of calix[4]arene (0.095 g, 0.22 mmol) in benzene- $d_6$  (0.50 mL) in a screw top NMR tube was added a solution of  $\text{Ge}[\text{N}(\text{SiMe}_3)_2]_2$  (0.088 g, 0.22 mmol) in benzene- $d_6$  (0.25 mL). The <sup>1</sup>H NMR spectrum was recorded 30 min after mixing the sample. The NMR tube was subsequently opened in the glovebox and an additional solution of  $\text{Ge}[\text{N}(\text{SiMe}_3)_2]_2$  (0.043 g, 0.11 mmol) in benzene- $d_6$  (0.15 mL) was added. After the reaction mixture was mixed, the <sup>1</sup>H NMR spectrum of the sample was recorded. This process was repeated with further addition of  $\text{Ge}[\text{N}(\text{SiMe}_3)_2]_2$  (0.051 g, 0.13 mmol) to the tube.

**Synthesis of {Calix[8]} $\text{Ge}_4$  (**6**).** To a solution of calix[8]arene (0.252 g, 0.297 mmol) in benzene (20 mL) in a Schlenk tube was added a solution of  $\text{Ge}[\text{N}(\text{SiMe}_3)_2]_2$  (0.514 g, 1.31 mmol) in benzene (10 mL). The tube was sealed with a Teflon plug, and the reaction was heated at 85 °C in an oil bath for 48 h. The volatiles were removed in vacuo to yield an off-white solid, which was washed with hexane ( $3 \times 5$  mL) and subsequently recrystallized from hot benzene (10 mL) to yield **6** (0.298 g, 89%) as colorless crystals. <sup>1</sup>H NMR ( $\text{C}_6\text{D}_6$ , 25 °C):  $\delta$  7.26 (d,  $J = 7.5$  Hz, 1H, *meta*-H C(55)), 7.25 (d,  $J = 7.5$  Hz, 1H, *meta*-H C(15)), 7.09 (d,  $J = 7.5$  Hz, 1H, *meta*-H C(43)), 7.08 (d,  $J = 7.5$  Hz, 1H, *meta*-H C(85)), 6.95–

- (53) Lee, S. K.; Mackay, K. M.; Nicholson, B. K.; Service, M. *J. Chem. Soc., Dalton Trans.* **1992**, 1709–1716.
- (54) Anema, S. G.; Lee, S. K.; Mackay, K. M.; McLeod, L. C.; Nicholson, B. K.; Service, M. *J. Chem. Soc., Dalton Trans.* **1991**, 1209–1217.
- (55) Anema, S. G.; Lee, S. K.; Mackay, K. M.; Nicholson, B. K.; Service, M. *J. Chem. Soc., Dalton Trans.* **1991**, 1201–1208.
- (56) Foster, S. P.; Mackay, K. M. *J. Organomet. Chem.* **1982**, 238, C46–C48.
- (57) Gerlach, R. F.; Mackay, K. M.; Nicholson, B. K.; Robinson, W. T. *J. Chem. Soc., Dalton Trans.* **1981**, 80–84.
- (58) Wong, F. S.; Mackay, K. M. *J. Chem. Res., Synop.* **1980**, 180.
- (59) Gerlach, R. F.; Graham, B. W. L.; Mackay, K. M. *J. Organomet. Chem.* **1979**, 182, 285–298.
- (60) Whitmire, K. H.; Lagrone, C. B.; Churchill, M. R.; Fetting, J. C.; Robinson, B. H. *Inorg. Chem.* **1987**, 26, 3491–3499.
- (61) Anema, S. G.; Mackay, K. M.; Nicholson, B. K.; Van Tiel, M. *Organometallics* **1990**, 9, 2436–2442.
- (62) Anema, S. G.; Mackay, K. M.; Nicholson, B. K. *J. Chem. Soc., Dalton Trans.* **1996**, 3853–3858.
- (63) Duffy, D. N.; Mackay, K. M.; Nicholson, B. K.; Thomson, R. A. *J. Chem. Soc., Dalton Trans.* **1982**, 1029–1034.
- (64) Evans, C.; Mackay, K. M.; Nicholson, B. K. *J. Chem. Soc., Dalton Trans.* **2001**, 1645–1649.
- (65) Lee, S. K.; Mackay, K. M.; Nicholson, B. K. *J. Chem. Soc., Dalton Trans.* **1993**, 715–722.
- (66) Foster, S. P.; Mackay, K. M.; Nicholson, B. K. *Inorg. Chem.* **1985**, 24, 909–913.
- (67) Foster, S. P.; Mackay, K. M.; Nicholson, B. K. *J. Chem. Soc., Chem. Commun.* **1982**, 1156–1157.
- (68) Gerlach, R. F.; Mackay, K. M. *J. Organomet. Chem.* **1979**, 178, C30–C32.
- (69) Lei, D.; Hampden-Smith, M. J.; Duesler, E. N.; Huffman, J. C. *Inorg. Chem.* **1990**, 29, 795–798.
- (70) Audett, J. A.; Mackay, K. M. *J. Chem. Soc., Dalton Trans.* **1988**, 2635–2643.
- (71) Bonny, A.; Mackay, K. M. *J. Chem. Soc., Dalton Trans.* **1978**, 1569–1573.
- (72) Elder, M.; Hutcheon, W. L. *J. Chem. Soc., Dalton Trans.* **1972**, 175–180.
- (73) Anema, S. G.; Barris, G. C.; Mackay, K. M.; Nicholson, B. K. *J. Organomet. Chem.* **1992**, 441, 35–43.
- (74) Anema, S. G.; Mackay, K. M.; Nicholson, B. K. *J. Organomet. Chem.* **1989**, 371, 233–246.
- (75) Anema, S. G.; Audett, J. A.; Mackay, K. M.; Nicholson, B. K. *J. Chem. Soc., Dalton Trans.* **1988**, 2629–2634.

- (76) Shriver, D. F.; Drezdson, M. A. *The Manipulation of Air Sensitive Compounds*, 2nd ed.; John Wiley and Sons: New York, 1986.
- (77) Harris, D. H.; Lappert, M. F. *J. Chem. Soc., Chem. Commun.* **1974**, 895–896.
- (78) Gynane, M. J. S.; Harris, D. H.; Lappert, M. F.; Power, P. P.; Rivière, P.; Rivière-Baudet, M. *J. Chem. Soc., Dalton Trans.* **1977**, 2004–2009.
- (79) Zhu, Q.; Ford, K. L.; Roskamp, E. J. *Heteroat. Chem.* **1992**, 3, 647–649.



6.85 (m, aromatics, 9 H), 6.79–6.91 (m, Ar 8 H), 6.66 (d,  $J = 7.5$  Hz, 1H, *meta*-H C(35)), 6.11 (t,  $J = 7.8$  Hz, 1H, *para*-H C(24)), 5.97 (d,  $J = 7.8$  Hz, 1H, *meta*-H C(25)), 5.83 (d,  $J = 16.8$  Hz, 2H, H(4a), H(8a)), 4.77 (d,  $J = 12.6$  Hz, 2H, H(1b), H(5b)), 4.60 (d,  $J = 15.8$  Hz, 2H, H(2b), H(3b)), 4.57 (d,  $J = 15.0$  Hz, 2H, H(6b), H(7b)), 3.46 (d,  $J = 15.8$  Hz, 2H, H(2a), H(3a)), 3.43 (d,  $J = 16.8$  Hz, 2H, H(4b), H(8b)), 3.41 (d,  $J = 15.0$  Hz, 2H, H(6a), H(7a)), 3.24 (d,  $J = 12.6$  Hz, 2H, H(1a), H(5a)) ppm.

**Synthesis of {Calix[8]}Ge<sub>4</sub>[Fe<sub>2</sub>(CO)<sub>8</sub>]<sub>4</sub> (7).** To a solution of **6** (0.150 g, 0.132 mmol) in benzene (15 mL) in a Schlenk tube was added a suspension of Fe<sub>2</sub>(CO)<sub>9</sub> (0.212 g, 0.583 mmol) in benzene (20 mL). The tube was sealed with a Teflon plug, and the mixture was heated at 85 °C for 24 h. The reaction mixture was filtered, and the solid was washed with benzene (4 × 10 mL) to yield a dark red filtrate. The volatiles were removed in vacuo to yield **7** as a dark-red solid (0.240 g, 73%). <sup>1</sup>H NMR (CD<sub>3</sub>CN, 25 °C):  $\delta$  7.13–6.97 (m, Ar 8H), 6.84–6.57 (m, Ar 18H), 4.70 (d,  $J = 10.2$  Hz, 8H, H(7b)), 4.12 (d,  $J = 12.9$  Hz, 8H, H(11a)), 3.72 (d,  $J = 12.9$  Hz, 8H, H(11b)), 3.43 (d,  $J = 10.2$  Hz, 8H, H(7a)). IR (CH<sub>2</sub>Cl<sub>2</sub>): 2109(w), 2059(s), 2044(m), and 2020(s) cm<sup>-1</sup>. UV (CH<sub>3</sub>-CN)  $\lambda_{\text{max}} = 327$  nm ( $\epsilon = 3.32 \times 10^4$ ).

**X-ray Structure Determinations.** Diffraction intensity data were collected with a Siemens P4/CCD diffractometer. Crystallographic data and details of the X-ray studies are shown in Table 4. Absorption corrections were applied for all data by SADABS. The structures were solved using direct methods, completed by Fourier syntheses, and refined by full-matrix least-squares procedures on  $F^2$ . All non-hydrogen atoms were refined with anisotropic displace-

**Table 4.** Crystallographic Data for Compounds **1**, **6**·C<sub>6</sub>H<sub>6</sub>, and **7**·C<sub>6</sub>H<sub>6</sub>

	<b>1</b>	<b>6</b> ·C <sub>6</sub> H <sub>6</sub>	<b>7</b> ·C <sub>6</sub> H <sub>6</sub>
formula	C <sub>28</sub> H <sub>20</sub> Ge <sub>2</sub> O <sub>4</sub>	C <sub>62</sub> H <sub>46</sub> Ge <sub>4</sub> O <sub>8</sub>	C <sub>94</sub> H <sub>46</sub> Fe <sub>8</sub> Ge <sub>4</sub> O <sub>40</sub>
space group	<i>Pbcn</i>	<i>P</i> $\bar{1}$	<i>P</i> 4(2)/ <i>n</i>
<i>a</i> (Å)	16.988(1)	12.923(4)	18.4671(6)
<i>b</i> (Å)	8.8914(7)	13.690(4)	18.4671(6)
<i>c</i> (Å)	14.630(1)	14.589(4)	15.956(1)
$\alpha$ (deg)	90	92.868(6)	90
$\beta$ (deg)	90	96.527(6)	90
$\gamma$ (deg)	90	93.774(6)	90
<i>V</i> (Å <sup>3</sup> )	2209.9(3)	2554(1)	5441.5(4)
<i>Z</i>	4	2	4
$\rho_{\text{calcd}}$ (g cm <sup>-3</sup> )	1.700	1.571	1.603
temp (K)	100(2)	198(2)	203(2)
radiation	Mo K $\alpha$	Mo K $\alpha$	Mo K $\alpha$
wavelength (Å)	0.71073	0.71073	0.71073
<i>R</i>	0.0290	0.0654	0.0476
<i>R</i> <sub>w</sub>	0.0626	0.1751	0.1528

ment coefficients, and hydrogen atoms were treated as idealized contributions. All software and sources of scattering factors are contained in the SHELXTL (5.10) program package (G. Sheldrick, Bruker XRD, Madison, WI). ORTEP diagrams were drawn using the ORTEP3 program (L. J. Farrugia, Glasgow).

**Acknowledgment.** We are grateful for the funding for this work which was provided by Oklahoma State University.

**Supporting Information Available:** Crystallographic data for compounds **1**, **6**, and **7** in CIF format. This information is available free of charge via the Internet at <http://pubs.acs.org>.

IC700969M